

Probability-Changing Cluster Algorithm: Study of Three-Dimensional Ising Model and Percolation Problem

Yusuke TOMITA* and Yutaka OKABE†

Department of Physics, Tokyo Metropolitan University, Hachioji, Tokyo 192-0397

(Received January 7, 2002)

We present a detailed description of the idea and procedure for the newly proposed Monte Carlo algorithm of tuning the critical point automatically, which is called the probability-changing cluster (PCC) algorithm [Y. Tomita and Y. Okabe, Phys. Rev. Lett. **86** (2001) 572]. Using the PCC algorithm, we investigate the three-dimensional Ising model and the bond percolation problem. We employ a refined finite-size scaling analysis to make estimates of critical point and exponents. With much less efforts, we obtain the results which are consistent with the previous calculations. We argue several directions for the application of the PCC algorithm.

KEYWORDS: Monte Carlo simulation, cluster algorithm, Ising model, percolation, finite-size scaling

1. Introduction

The Ising model¹⁾ is a basic model for studying phase transitions and critical phenomena. The q -state Potts model,^{2,3)} which has q components for the order parameter, is a generalization of the Ising model. Then, the Ising model corresponds to the $q = 2$ Potts model. The percolation model⁴⁾ also exhibits a geometric phase transition. The Kasteleyn-Fortuin (KF) cluster representation⁵⁾ of the q -state Potts model bridges the Potts model and the percolation problem; the bond percolation problem can be regarded as the $q = 1$ Potts model. Recently, based on the cluster formalism, the multiple-percolating clusters of the Ising system with large aspect ratio have been studied.⁶⁾

For two-dimensional (2D) systems, exact or rigorous results have been obtained for the Potts models,^{7,8)} and they are used as the testing ground for numerical study. On the other hand, for three-dimensional (3D) systems, it is rare that exact results are available, and we rely more on numerical studies for revealing the nature of the problem. The Monte Carlo simulation⁹⁾ is a standard powerful tool to study critical phenomena numerically. To obtain accurate data, the development of efficient algorithms is highly demanded. Cluster algorithms^{10,11)} are examples of such efforts, and they have been successfully used to overcome slow dynamics in the Monte Carlo simulation. Swendsen and Wang (SW)¹⁰⁾ applied the KF⁵⁾ representation to identify clusters of spins.

Extending the SW algorithm, we have recently proposed an effective cluster algorithm of tuning the critical point automatically; this algorithm is called the probability-changing cluster (PCC) algorithm.¹²⁾ We have shown the effectiveness of the PCC algorithm for the case of 2D Potts models in the Letter.¹²⁾ The basic idea of our algorithm is that we change the probability of connecting parallel spins p in the KF representation during the process of the Monte Carlo spin update. We decrease or increase p depending on the observation whether the KF clusters are percolating or not percolating; essentially, we change the temperature. This simple

negative feedback mechanism together with the finite-size scaling (FSS)¹³⁾ property of the existence probability (also called the crossing probability) E_p , the probability that the system percolates, leads to the determination of the critical point. Since our ensemble is asymptotically canonical as Δp , the amount of the change of p , becomes 0, the distribution functions of physical quantities obey the FSS; as a result, we can determine critical exponents using the FSS analysis.

Previously, Machta *et al.*¹⁴⁾ proposed another idea of cluster algorithm to tune the critical point automatically, which is called the invaded cluster (IC) algorithm. However, the ensemble of the IC algorithm is not necessarily clear, and it has a problem of “bottlenecks”, which causes the broad tail in the distribution of the fraction of the accepted satisfied bonds.¹⁴⁾ In contrast, it is guaranteed that we approach the canonical ensemble in our PCC algorithm.

In this paper we give the more detailed description of the PCC algorithm, and show the results for the 3D Ising model and the 3D bond percolation problem. We pay attention to the refined FSS analysis for determining the critical point and critical exponents, which is the same idea as was used in a high-resolution Monte Carlo study by Ferrenberg and Landau.¹⁷⁾ The rest of this paper is organized as follows: In §2 we explain the idea and the procedure of the PCC algorithm. In §3 the results for the 3D Ising model and percolation problem are shown, and the refined FSS analysis is discussed. Finally, we summarize this paper and give discussions in §4.

2. Probability-Changing Cluster Algorithm

2.1 Idea of PCC algorithm for Ising model

We start with explaining the idea of the PCC algorithm. Here, we deal with the ferromagnetic Ising model, whose Hamiltonian is given by

$$\mathcal{H} = -J \sum_{\langle i,j \rangle} \sigma_i \sigma_j, \quad \sigma_i = \pm 1, \quad (2.1)$$

where J is the exchange coupling constant, and the summation is taken over the nearest-neighbor pairs $\langle i, j \rangle$. In this case, the probability of connecting parallel spins in the KF representation is given by $p = 1 - e^{-2J/k_B T}$. The procedure of Monte Carlo spin update is as follows:

1. Start from some spin configuration and some value of p .
2. Make KF clusters using the probability p , and check whether the system is percolating or not. Update spins following the same rule as the SW algorithm, that is, flip all the spins on any KF cluster to one of two states.
3. If the system is percolating (not percolating) in the previous test, decrease (increase) p by Δp (> 0). Essentially, we change the temperature T .
4. Go back to the process 2.

Since we use the cluster representation and assign clusters, we are ready to check whether the system is percolating or not in the process 2. The distribution of p for Monte Carlo samples approaches the Gaussian distribution of which mean value is $p_c(L)$, after repeating the above processes. Here, $p_c(L)$ is the probability of connecting spins, such that the existence probability E_p becomes 1/2, and depends on the system size L . The existence probability E_p is the probability that the system percolates. In the limit of $\Delta p \rightarrow 0$, we approach the canonical ensemble, which will be discussed later. Then, we can use the FSS analysis. We should note that E_p follows the FSS near the critical point,

$$E_p(p, L) \sim X(tL^{1/\nu}), \quad t = (p_c - p)/p_c, \quad (2.2)$$

as far as the corrections to FSS are negligible, where p_c is the critical value of p for the infinite system ($L \rightarrow \infty$) and ν is the correlation-length critical exponent. Then, we can estimate p_c from the size dependence of $p_c(L)$ using eq. (2.2) and, in turn, estimate T_c through the relation $p_c = 1 - e^{-2J/k_B T_c}$.

2.2 Percolating condition

There are several choices of criterion to determine percolating. For example, Machta *et al.*¹⁴⁾ used both the extension rule and the topological rule for their stopping condition in the IC algorithm. The former rule is that some cluster has maximum extent L in at least one of the d directions in d -dimensional systems. The latter rule is that some cluster winds around the system in at least one of the d directions. We may use these percolating conditions in our PCC algorithm. Actually, we can use any rule to determine percolating, but FSS functions for physical quantities, therefore $p_c(L)$, depend on the rule.

2.3 Distribution of p

Let us consider the distribution of p , $f(p)$. We change p based on the observation whether the system is percolating or not, which leads to the negative feedback mechanism. Since the existence probability $E_p(p)$ is the probability that the systems percolates, the transition probabilities W from p to $p + \Delta p$ and from p to $p - \Delta p$

in the PCC algorithm are written as follows:

$$\begin{cases} W_{p \rightarrow p + \Delta p} = 1 - E_p(p), \\ W_{p \rightarrow p - \Delta p} = E_p(p). \end{cases} \quad (2.3)$$

In the vicinity of $p_c(L)$, we may employ the linear approximation for $E_p(p)$, such as

$$E_p(p) = \frac{1}{2} + a(p - p_c(L)), \quad (2.4)$$

where a is the value of dE_p/dp at $p_c(L)$. Then, this problem is nothing but the Ehrenfest model for *diffusion with a central force*.^{15, 16)} In the steady state, the distribution of p , $f(p)$, satisfies the relation

$$f(p) = W_{p - \Delta p \rightarrow p} f(p - \Delta p) + W_{p + \Delta p \rightarrow p} f(p + \Delta p). \quad (2.5)$$

In the linear approximation, eq. (2.4), p takes the values between $p_c(L) - 1/2a$ and $p_c(L) + 1/2a$. Substituting eqs. (2.3) and (2.4) into eq. (2.5) and denoting $p = p_c(L) + i\Delta p$, we can show that $f(p)$ is the binomial distribution, that is,

$$f(p) \propto {}_n C_{n/2+i}, \quad (2.6)$$

where $n = (1/a)/\Delta p$, $i \in [-n/2, n/2]$, and ${}_n C_{n/2+i}$ are the binomial coefficients. Thus, for large n , or small Δp , the distribution function $f(p)$ becomes the Gaussian distribution with the average $p_c(L)$ and the variance $\sigma^2 = (n/4)(\Delta p)^2 = \Delta p/4a$. For smaller Δp , the width of the distribution becomes narrower as $\sigma \propto \sqrt{\Delta p}$. Since a is the value of dE_p/dp at $p_c(L)$, we expect $a \propto L^{1/\nu}$ using the FSS assumption, eq. (2.2). Thus, for larger L , the width of $f(p)$ becomes narrower.

In the Letter,¹²⁾ we have checked that the distribution of p actually approaches the Gaussian distribution with very narrow width for the 2D Ising model, and the resulting energy histogram is indistinguishable from that by the constant-temperature calculation. Moreover, we have obtained the expected Δp - and L -dependence for the width of $f(p)$.

2.4 Determination of next p

In the process 3, we decrease or increase p by Δp . The difference Δp is a free parameter in our algorithm. In the limit of small Δp we approach the canonical ensemble, but it takes a long time to equilibrate for small Δp . Using the same approximation as in the previous subsection and assuming that the subsequent steps are independent, we can show that the deviation of the average value of p from $p_c(L)$ becomes smaller as a geometric progression with time. Since the geometric ratio is given by $1 - 2a\Delta p$ in this approximation, the convergence becomes slower for smaller Δp . Practically, we may start with rather large Δp , and gradually decrease Δp with monitoring the trail of the values of p . Small steps of preparation are enough for equilibration.

We change p by every Monte Carlo step in our original proposal.¹²⁾ As another way, we may measure the existence probability E_p for a short time interval with keeping p constant, and then change p for the next short

time interval. In this process, recording the values of p and whether percolation occurred for each, we may extract the information on the final $p_c(L)$ efficiently using the Bayesian statistics.¹⁸⁾ A more deterministic way of adjusting $p_c(L)$ may be considered. Solving $E_p(p) = 1/2$ iteratively by the Newton method may lead to the adjustment of $p_c(L)$.¹⁹⁾ It is quite interesting to improve and extend the method of PCC algorithm.

2.5 Checking value of E_p

We have chosen the value of E_p which gives $p_c(L)$ as $1/2$ because it is the simplest. In case the critical value of E_p at the critical point of the infinite system is far from $1/2$, it is convenient to employ the checking value of E_p different from $1/2$. We may modify the update process such that this value is different from $1/2$. If we want to choose the checking value of E_p as e_p , we may modify the process 3 as follows:

- 3'. If the system is percolating in the previous test, decrease p by Δp with the probability $s = \min[(1/2)/e_p, 1]$ and increase p with the probability $1 - s$. On the contrary, if the system is not percolating, increase p by Δp with the probability $s' = \min[(1/2)/(1 - e_p), 1]$ and decrease p with the probability $1 - s'$.

In this way, we can control the checking value of E_p .

3. Results

3.1 3D Ising model

Here we present the result of the 3D Ising model. We have simulated the Ising model on the simple cubic lattice by using the PCC algorithm. We have treated the systems with linear sizes $L=8, 12, 16, 24, 32, 48$, and 64. For the criterion to determine percolating, we have employed the topological rule¹⁴⁾ in the present study. After 10,000 Monte Carlo sweeps of determining $p_c(L)$ with gradually reducing Δp , we have made 100,000 Monte Carlo sweeps to take the thermal average; we have made 10 runs for each size to get better statistics and to evaluate the statistical errors. We have started with $\Delta p = 10^{-3}$ for $L = 8$ and $\Delta p = 10^{-4}$ for $L = 64$. For the intermediate sizes, we have started with Δp between these two values. The final value of Δp has been chosen as $\Delta p = 10^{-5} \times L^{-1.6}$ for the system size L . Actually, the schedule of decreasing Δp is not so serious.

We plot the size-dependent $T_c(L)$ as a function of $1/L$ for the 3D Ising model in Fig. 1. From now on, we represent the temperature in units of J/k_B . The error bars are within the size of the mark. The critical temperature T_c can be estimated by the FSS relation, eq. (2.2). Including the corrections to FSS, we have

$$T_c(L) = T_c + aL^{-1/\nu}(1 + bL^{-\omega}), \quad (3.1)$$

where $T_c(L)$ is given through $p_c(L) = 1 - e^{-2J/k_B T_c(L)}$, and ω is the correction-to-FSS exponent. Since there are five fitting parameters in eq. (3.1), it is not easy to get accurate estimates of the critical point and critical exponents. In a high-resolution Monte Carlo study, Ferrenberg and Landau¹⁷⁾ employed a FSS analysis to get

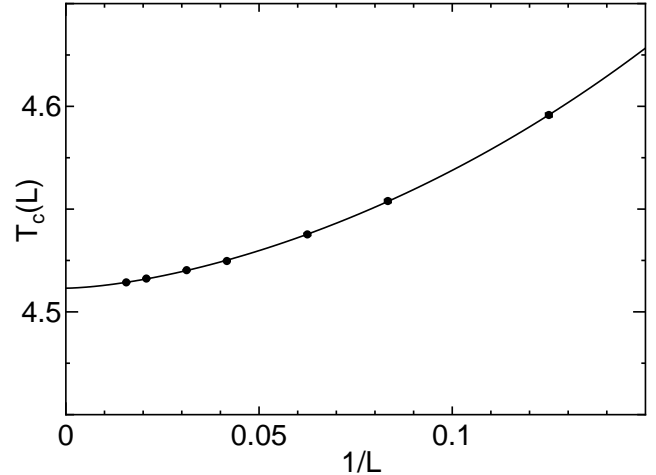


Fig. 1. Plot of $T_c(L)$ (in units of J/k_B) as a function of $1/L$ for the 3D Ising model. The system sizes are $L = 8, 12, 16, 24, 32, 48$, and 64.

accurate estimates. They first determine the exponent ν , and with ν determined quite accurately they then estimate T_c . Since their procedure is well fitted for our algorithm, we use the same idea.

We first note that the inverse-temperature derivatives of the logarithm for the moment of magnetization m obey the following FSS relations,

$$\frac{\partial \ln \langle m^n \rangle}{\partial K} = a' L^{1/\nu} (1 + b' L^{-\omega}), \quad (3.2)$$

where $K = 1/k_B T$ and $\langle \cdots \rangle$ denotes the thermal average. These FSS relations hold for the values of m at the size-dependent $T_c(L)$ as well as those at the fixed T_c for the infinite system. Here, we treat the variables at $T_c(L)$. Since we calculate the left-hand side of eq. (3.2) by the general formula to calculate the K -derivative of any quantity $\langle A \rangle$,

$$\frac{\partial \langle A \rangle}{\partial K} = \langle A \rangle \langle E \rangle - \langle AE \rangle, \quad (3.3)$$

where E is the energy, we can extract ν without determining T_c for the infinite system. The inverse-temperature derivative of the Binder parameter,²⁰⁾ which is defined as

$$g = \frac{1}{2} \left(3 - \frac{\langle m^4 \rangle}{\langle m^2 \rangle^2} \right), \quad (3.4)$$

also obeys the FSS relation as in eq. (3.2). What we do is that we measure the inverse-temperature derivatives of $\ln \langle m^n \rangle$ and g at the size-dependent $T_c(L)$ and make an analysis based on the FSS relations, eq. (3.2).

We plot the derivatives $\partial g / \partial K$, $\partial \ln \langle |m| \rangle / \partial K$ and $\partial \ln \langle m^2 \rangle / \partial K$ at $T_c(L)$ as a function of L in logarithmic scale in Fig. 2. The error bars are again within the size of the mark. We find the power-law size dependence from the linearity of the data with small corrections to FSS; we estimate the exponent $1/\nu = 1.594(8)$ using eq. (3.2). Here, the number in the parenthesis denotes the uncertainty in the last digit. We have used the average of three

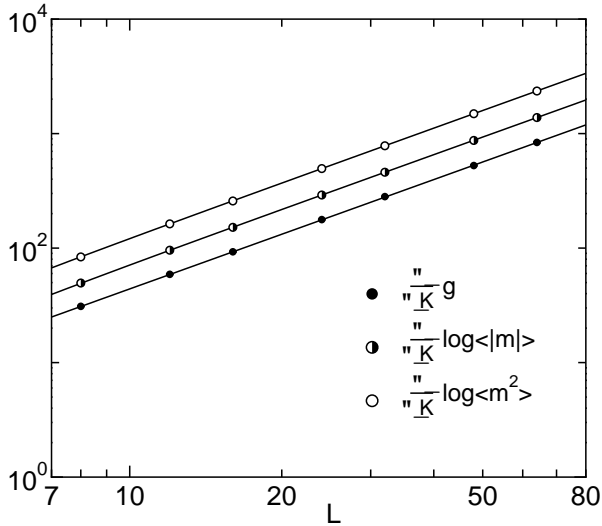


Fig. 2. Plot of derivatives at $T_c(L)$ as a function of L for the 3D Ising model in logarithmic scale.

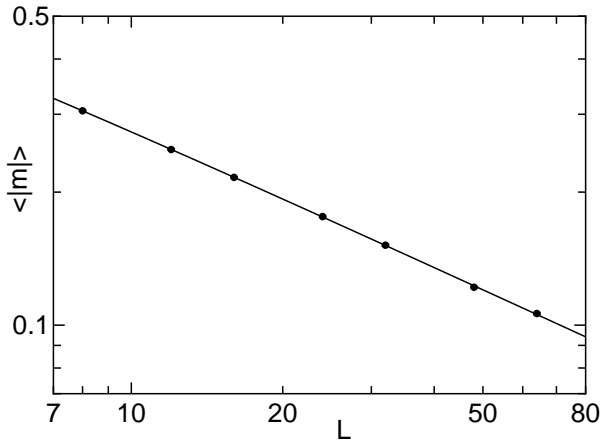


Fig. 3. Plot of $\langle |m| \rangle$ at $T_c(L)$ as a function of L for the 3D Ising model in logarithmic scale.

data. The correction-to-FSS exponent ω is $1.2(5)$, which is a little bit larger than the recent value $\omega = 0.87(9)$.²¹⁾ Our estimate of T_c using eq. (3.1) is $T_c = 4.5108(7)$, that is, $1/T_c = 0.22169(4)$. Both estimates of T_c and ν are consistent with the estimates of the recent study,¹⁷⁾ $1/\nu = 1.590(2)$ and $1/T_c = 0.2216595(26)$. The solid curve in Fig. 1 is the best fitted curve for eq. (3.1) with ν determined accurately first.

In order to discuss another exponent, we plot the average of the magnetization $\langle |m| \rangle$ at $T_c(L)$ as a function of L in logarithmic scale in Fig. 3. We use the FSS relation with the corrections to FSS,

$$\langle |m| \rangle_{T=T_c(L)} = cL^{-\beta/\nu}(1 + dL^{-\omega}), \quad (3.5)$$

for the estimate of the magnetization exponent β . From the least square fit using eq. (3.5), we have $\beta/\nu = 0.517(8)$, which is again consistent with the recent estimate,¹⁷⁾ $\beta/\nu = 0.518(7)$.

It is interesting to study the distribution function of physical quantities. We show the FSS plot of the dis-

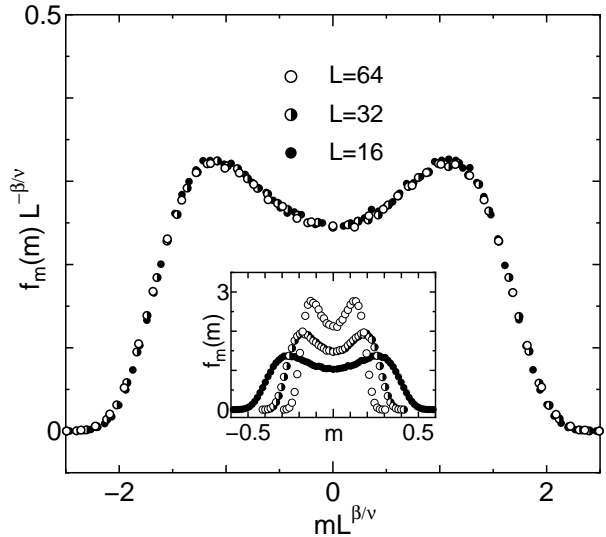


Fig. 4. FSS plot of $f_m(m)$ for the 3D Ising model, where $\beta/\nu = 0.517$. The system sizes are $L = 16, 32$, and 64 . The inset shows the raw data.

tribution function $f_m(m)$ in Fig. 4, based on the FSS relation,

$$f_m(m)_{T=T_c(L)} \sim L^{\beta/\nu} h(mL^{\beta/\nu}). \quad (3.6)$$

The inset of Fig. 4 shows the raw data of the distribution functions $f_m(m)$ for linear sizes $L = 16, 32$, and 64 . The scaled data show very good FSS behavior; that is, the data of different sizes are collapsed on a single curve.

3.2 3D bond percolation problem

The idea of the PCC algorithm is based only on the property of a percolation problem. Thus, it is straightforward, or even easier, to apply this algorithm to the geometric percolation problem. The partition function for the bond percolation problem is written as

$$Z = \sum_{G' \subseteq G} p^{b(G')} (1-p)^{N_b - b(G')}. \quad (3.7)$$

Here G is all the configurations, or the graph, and $b(G')$ is the number of occupied bonds in the subgraph G' . The sum is over all subgraphs G' of G . The probability of bond occupation is denoted by p , and N_b is the total number of bonds in the system. In the bond percolation problem, we are to locate the percolation threshold p_c . We change p by the small amount of Δp in the process of simulation, and determine the size-dependent $p_c(L)$ automatically as in the case of the Ising model. In the limit of $\Delta p \rightarrow 0$, it becomes the usual percolation problem. One thing we should have in mind is that we determine whether the bond is occupied or not with the probability p for each bond.

We have studied the 3D bond-percolation model with linear sizes $L = 8, 12, 16, 24, 32, 48$, and 64 . Almost the same conditions are used as in the 3D Ising model. We plot the size-dependent $p_c(L)$ as a function of $1/L$ in Fig. 5. The FSS relation for $p_c(L)$ is given by the equation similar to eq. (3.1), but we follow the same scheme

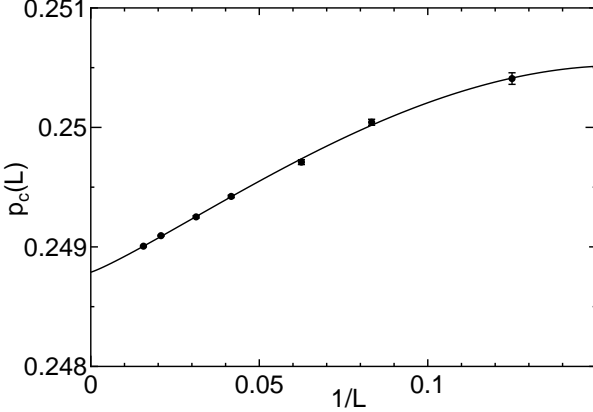


Fig. 5. Plot of $p_c(L)$ as a function of $1/L$ for the 3D bond percolation problem. The system sizes are $L = 8, 12, 16, 24, 32, 48$, and 64 .

as in the Ising model to get better estimates of the critical point and exponents; that is, we first estimate the critical exponent ν . The fraction of lattice sites in the largest cluster c plays a role of the order parameter. Thus, we consider the p -derivative of the moments of c . The derivative of any quantity $\langle A \rangle$ with respect to p is given by

$$\frac{\partial \langle A \rangle}{\partial p} = \frac{\langle Ab \rangle - \langle A \rangle \langle b \rangle}{p(1-p)}, \quad (3.8)$$

where b is the number of occupied bonds, and $\langle \dots \rangle$ denotes the sample average. Equation (3.8) corresponds to the general formula for the K -derivative, eq. (3.3). We may derive eq. (3.8) starting from the expression for the partition function, eq. (3.7), or using the correspondence based on the KF relation, $p = 1 - e^{-2J/k_B T}$.

We have calculated the logarithmic derivatives of $\langle c \rangle$ and $\langle c^2 \rangle$, where c is the fraction of lattice sites in the largest cluster. Since the moment ratio $\langle c \rangle^2 / \langle c^2 \rangle$ has the same FSS property as the Binder parameter, eq. (3.4), we also calculate the p -derivative of this moment ratio. We plot the derivatives $\partial(\langle c \rangle^2 / \langle c^2 \rangle) / \partial p$, $\partial \ln \langle c \rangle / \partial p$ and $\partial \ln \langle c^2 \rangle / \partial p$ at $p_c(L)$ as a function of L in logarithmic scale in Fig. 6. We find the power-law size dependence from the linearity of the data with small corrections to FSS; we estimate the exponent $1/\nu = 1.12(5)$ from the slopes of lines. The correction-to-FSS exponent ω is $1.1(5)$, which is a little bit smaller than the recent estimate for site percolation problem, $\omega = 1.62(13)$.²¹⁾ We can use the FSS form similar to eq. (3.1) for the estimate of p_c ; our estimate using the value of ν is $p_c = 0.24881(3)$. Both estimates of p_c and ν are consistent with the estimates of the recent study,²²⁾ $1/\nu = 1.12(3)$ and $p_c = 0.2488126(5)$. The solid curve in Fig. 5 is the best fitted curve for p_c , which is similar to eq. (3.1), with ν determined accurately first.

We plot the fraction of lattice sites in the largest cluster $\langle c \rangle$ at $p_c(L)$ as a function of L in logarithmic scale in Fig. 7. Since $\langle c \rangle$ has the same FSS form as the magnetization, we use eq. (3.5) for the estimate of β/ν . Using the least square fit, we have $\beta/\nu = 0.474(5)$, which is again consistent with the estimate of recent study,²²⁾

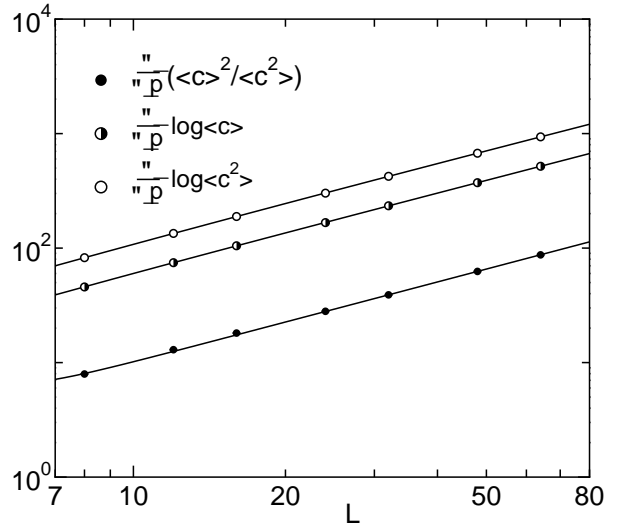


Fig. 6. Plot of derivatives at $p_c(L)$ as a function of L for the 3D bond percolation problem in logarithmic scale.

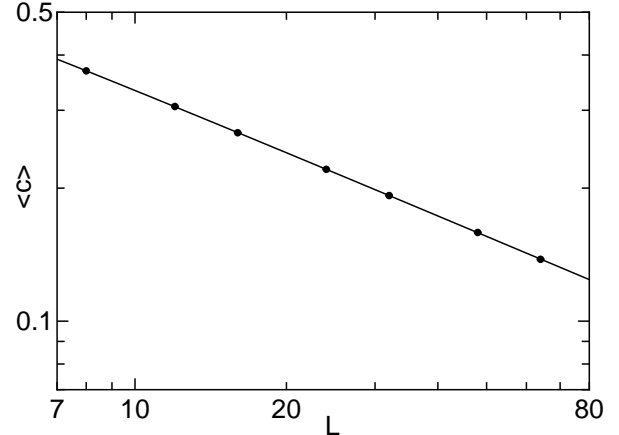


Fig. 7. Plot of $\langle c \rangle$ at $p_c(L)$ as a function of L for the 3D bond percolation problem in logarithmic scale.

$$\beta/\nu = 0.476(5).$$

Finally, we show the FSS plot of the distribution function $f_c(c)$ in Fig. 8. The raw data of $f_c(c)$ for linear sizes $L = 16, 32$, and 64 are given in the inset of Fig. 8. Again, in the percolation problem, the data show very good FSS behavior.

4. Summary and Discussions

To summarize, we have given a detailed description of the newly proposed PCC algorithm. We have applied the PCC algorithm to the study of the 3D Ising model and the 3D bond percolation problem. We have employed a refined analysis of FSS, which uses the same scheme as suggested by Ferrenberg and Landau.¹⁷⁾ Our results for the Ising model and the bond percolation problem are consistent with those of the previous works.^{17, 22)} It is to be noted that we make simulations at a single critical point $p_c(L)$ for each system size. Thus, we need much less efforts compared with the usual procedure for making simulations at several different temperatures to

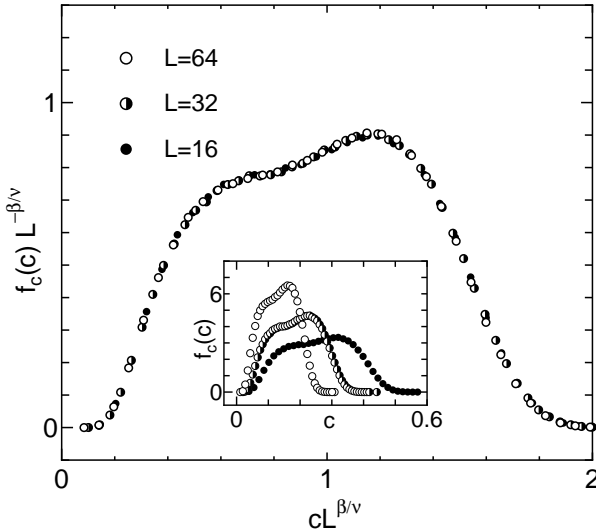


Fig. 8. FSS plot of $f_c(c)$ for the 3D bond percolation problem, where $\beta/\nu = 0.474$. The system sizes are $L = 16, 32$, and 64 . The inset shows the raw data.

extract the critical point and to estimate critical exponents.

We have estimated ν from the temperature derivative of the moments. There is an alternative way to estimate ν without determining T_c . Let us calculate the size-dependent T_c in two ways. We may use different criteria for percolating condition; we may use different values of E_p which gives $p_c(L)$. Then, the difference of two $T_c(L)$'s follows the FSS relation as

$$T_c^{(1)}(L) - T_c^{(2)}(L) = a'' L^{-1/\nu} (1 + b'' L^{-\omega}), \quad (4.1)$$

which also leads to the direct determination of ν .

There are several directions for the application of the PCC algorithm. We can use the PCC algorithm to any problem where the mapping to the cluster formalism exists. It is straightforward to apply this algorithm to the diluted Ising (Potts) models. The PCC algorithm is quite useful for investigating the self-averaging properties of random systems, where the distribution of T_c due to randomness is essential. It is because we can determine the sample-dependent $p_c(L)$ quite easily. We have already applied the PCC algorithm to the 2D site-diluted Ising model,²³⁾ and have studied the crossover and self-averaging properties. It is also interesting to extend the PCC algorithm to the problem of the vector order parameter. We have already succeeded in applying the PCC algorithm to the classical XY model,²⁴⁾ and have shown that the PCC algorithm is useful not only for the analysis of the second-order transition but also for that of the transition of the Kosterlitz-Thouless type.

In the PCC algorithm, the cluster representation is used in two ways. First, we make a cluster flip as in the SW algorithm.¹⁰⁾ Second, we change p depending on the observation whether clusters are percolating or not. However, the percolating properties are not essen-

tial. We have used the FSS relation for E_p , eq. (2.2), to determine the critical point. We may use quantities other than E_p which have the similar FSS relation with

a single scaling variable. We could generalize the PCC algorithm for a problem where the mapping to the cluster formalism does *not* exist. For example, we may study the systems with a frustration by the generalized scheme of the PCC algorithm. The application of the PCC algorithm to quantum spin systems is also an interesting subject, and now in progress.

Acknowledgments

We thank N. Kawashima, H. Otsuka, M. Kikuchi, R. H. Swendsen, and J.-S. Wang for valuable discussions. The computation in this work has been done using the facilities of the Supercomputer Center, Institute for Solid State Physics, University of Tokyo. This work was supported by a Grant-in-Aid for Scientific Research from the Japan Society for the Promotion of Science.

- 1) E. Ising: *Z. Phys.* **31** (1925) 253.
- 2) R. B. Potts: *Proc. Camb. Phil. Soc.* **48** (1952) 106; T. Kihara, Y. Midzuno and T. Shizume: *J. Phys. Soc. Jpn.* **9** (1954) 681.
- 3) F. Y. Wu: *Rev. Mod. Phys.* **54** (1982) 235 and references therein.
- 4) D. Stauffer and A. Aharony: *Introduction to Percolation Theory*, Revised 2nd ed. (Taylor and Francis, London, 1994).
- 5) P. W. Kasteleyn and C. M. Fortuin: *J. Phys. Soc. Jpn. Suppl.* **26** (1969) 11; C. M. Fortuin and P. W. Kasteleyn: *Physica* **57** (1972) 536.
- 6) Y. Tomita, Y. Okabe and C.-K. Hu: *Phys. Rev. E* **60** (1999) 2716.
- 7) L. Onsager: *Phys. Rev.* **65** (1949) 117.
- 8) P. D. Beale: *Phys. Rev. Lett.* **76** (1996) 78.
- 9) D. P. Landau and K. Binder: *A Guide to Monte Carlo Simulations in Statistical Physics*, (Cambridge University Press, Cambridge, 2000).
- 10) R. H. Swendsen and J. S. Wang: *Phys. Rev. Lett.* **58** (1987) 86.
- 11) U. Wolff: *Phys. Rev. Lett.* **62** (1989) 361.
- 12) Y. Tomita and Y. Okabe: *Phys. Rev. Lett.* **86** (2001) 572.
- 13) M. E. Fisher: in *Critical Phenomena, Proceedings of the International School of Physics "Enrico Fermi"*, edited by M. S. Green (Academic, New York, 1971), Vol. 51, p. 1; in *Finite-size Scaling*, edited by J. L. Cardy (North-Holland, New York, 1988).
- 14) J. Machta, Y.-S. Choi, A. Lucke, T. Schweizer and L. V. Chayes: *Phys. Rev. Lett.* **75** (1995) 2792; *Phys. Rev. E* **54** (1996) 1332.
- 15) P. Ehrenfest and T. Ehrenfest: *Phys. Z.* **8** (1907) 311.
- 16) W. Feller: *An Introduction to Probability Theory and Its Application*, Vol. 1, 3rd ed. (John Wiley & Sons, New York, 1968).
- 17) A. M. Ferrenberg and D. P. Landau: *Phys. Rev. B* **44** (1991) 5081.
- 18) R. H. Swendsen: private communication.
- 19) J. S. Wang: private communication.
- 20) K. Binder: *Z. Phys. B* **43** (1981) 119.
- 21) H. G. Ballesteros, L. A. Fernández, V. Martin-Mayor, A. Muñoz Sudupe, G. Parisi and J. J. Ruiz-Lorenzo: *J. Phys. A* **32** (1999) 1.
- 22) C. D. Lorenz and R. M. Ziff: *Phys. Rev. E* **57** (1998) 230.
- 23) Y. Tomita and Y. Okabe: *Phys. Rev. E* **64** (2001) 036114.
- 24) Y. Tomita and Y. Okabe: *Phys. Rev. B*, to appear.